Nutcracker Optimization Algorithm to Address Power System's Optimal Power Flow Issue

Xun Liu, Jun-Hua Zhu, Jie-Sheng Wang*, Song-Bo Zhang, Xin-Yi Guan

Abstract—**The optimal power flow (OPF) in electrical power systems focuses on optimizing objective parameters such as generating costs by altering control factors while remaining within operational restrictions and supply-demand balance. Grid power balance, specifically the upper and lower bounds of generator power exports, and the upper limit of reactive power compensator capacity are all employed as constraints in the optimal power flow problem, and a mathematical model of the problem is developed. The Nutcracker Optimization Algorithm (NOA) is implemented to resolve the optimal power flow issue, which is then assessed an IEEE-30 bus system.The objective functions used for this study encompass generating cost, active power losses, voltage stability, and bus voltage variations. The results were then compared to those obtained using Gray Wolf Optimizer (GWO), Sand Cat Swarm Optimization (SCSO), Whale Optimization Algorithm (WOA), and Dung Beetle Optimizer (DBO). The NOA can indeed deal with the optimal power flow problem, as the simulation results show.**

Index Terms—**optimal power flow, nutcracker optimization algorithm, constrained optimization, electric network**

I. Introduction

Optimal power flow (OPF) is a critical strategy for ensuring economic and secure operation of the electricity grid. It's also the fundamental component of the energy governance framework, the essence of which refers to the optimization of one or more performance indicators characterizing the level of grid operation by adjusting the control equipment, given the system structural parameters and loads. The optimal OPF issue is a nonlinear, non-convex, and extremely complex optimization challenge that includes both continuous and discontinuous control variables.

Manuscript received March 24, 2024; revised June 20, 2024. This work was supported by the Basic Scientific Research Project of Institution of Higher Learning of Liaoning Province (Grant No. LJKZ0293), and Postgraduate Education Reform Project of Liaoning Province (Grant No. LNYJG2022137).

Xun Liu is a postgraduate student of School of Electronic and Information Engineering, University of Science and Technology Liaoning, Anshan, 114051, P. R. China (e-mail: heidengxiaguo@163.com).

Jun-Hua Zhu is a postgraduate student of School of Electronic and Information Engineering, University of Science and Technology Liaoning, Anshan, 114051, P. R. China (e-mail: zhujunhua1999@163.com).

Jie-Sheng Wang is a professor of School of Electronic and Information Engineering, University of Science and Technology Liaoning, Anshan, 114051, P. R. China (Corresponding author, phone: 86-0412-2538246; fax: 86-0412-2538244; e-mail: wang_jiesheng@126.com).

Song-Bo Zhang is a postgraduate student of School of Electronic and Information Engineering, University of Science and Technology Liaoning, Anshan, 114051, P. R. China (e-mail: 2092926911@qq.com).

Xin-Yi Guan is a postgraduate student of School of Electronic and Information Engineering, University of Science and Technology Liaoning, Anshan, 114051, P. R. China (e-mail: a18524333171@163.com).

A wide range of optimization strategies have been used to meet the OPF difficulty.These methods are roughly categorized into two types: traditional optimization approaches and meta-heuristic algorithms. The former include linear programming (LP) [3], quadratic programming (QP) [4], sequential programming [5], newton's method [6], nonlinear programming [7-8], mixed integer nonlinear programming (MINLP) [9], interior point method (IPM) [10-11], simplified gradient method (SGM) [12], and other mathematical optimization methods. In these traditional methods, due to the inability of the mathematical methods to deal with the nonlinear nature, the nonlinear objective function and constraints must be converted to a linear form [13]. Such alterations can have an impact on the accuracy with which power systems are operated and planned. These approaches face three main obstacles. To begin, the ideal Power Flow (OPF) problem often contains numerous local optima, and standard methods may fail to produce the ideal solution, instead converging to a local optimum. Second, these methods need the continuity and differentiability of the goal function, which is not always possible in real-world systems. Finally, these methods are not appropriate for discrete variables like transformer tap settings.

To circumvent the constraints of standard mathematical optimization methods, various successful metaheuristic algorithms have been devised based on biological behavior. Inspired by their origins, these algorithms fall into two classes: evolutionary algorithms and swarm intelligence algorithms. Evolutionary algorithms are those that model natural evolutionary processes. Ref. [14] describes a combination of genetic algorithm and Matpower. Simple behaviors that mimic social organisms are classified as swarm intelligence algorithms. Ref. [15] describes an effective whale optimization algorithm (EWOA) that introduces Lévy motion to encircle prey and Brownian motion to search for prey to improve the ability to explore the globe and maintain an appropriate balance between exploration and exploitation. In Ref. [16], swarm algorithms are utilized to tackle OPF challenges for hybrid systems. In addition, there are many hybrid meta-heuristic algorithms. In Ref. [17], an updated JAYA algorithm was used to settle the OPF issue in a test system using renewable power options. This revised JAYA algorithm successfully addressed the OPF problem in such a system. In Ref. [18], a stack planning method was used to tackle the OPF problem for solar and wind energy. This study looked at photovoltaic panels, power plants, and daily load curves, and used the stack planning algorithm to solve the OPF problem. Ref. [19] used a hybrid approach to tackle the OPF problem. A hybrid algorithm called DA-PSO, which

combines the Dragonfly Algorithm (DA) with Particle Swarm Optimization (PSO), was applied. This hybrid approach used the exploration and exploitation stages of the DA and PSO algorithms, to settle multi-objective OPF issue. Ref. [20] utilized a hybrid Firefly Particle Swarm Optimization (HFPSO) algorithm to address various nonlinear and non-convex OPF issue.

Nutcracker optimization algorithm (NOA) is a new optimization algorithm presented by Abdel-Basset Mohamed and Reda Mohamed et al. in 2023 [21], which is inspired by Clark's nutcracker, which is distributed in the mountains of the western United States and Canada. Compared to other meta-heuristic algorithms, NOA uses different local and global search operators and introduces more positional information to make better use of the exploration domain, which enables it to solve problems in a better way.In this study, the NOA is employed to address the OPF problem. This method's effectiveness was confirmed initially with CEC2017 test functions before being applied to the IEEE-30 bus system. The findings showed that NOA is an effective strategy for treating OPF issues.

The second section contains the mathematical formulation for the Optimal Power Flow (OPF) model. The third section outlines the IEEE-30 bus power grid and the targets to be optimized. Section IV introduces the NOA. Section V evaluates the NOA's performance using the CEC2017 benchmark functions. Section VI outlines the objective functions to be employed in the simulation experiments on the IEEE-30 bus system. Finally, Section VII offers a synthesis of the preceding sections and presents a concluding remark.

II. Mathematical Model of Optimal Power Flow Problem

The Optimal Power Flow (OPF) issue aims to identify an arrangement of control parameters which minimize the specified objective operates while adhering to particular equality and non-equality restrictions. The mathematical formulation of the OPF is described below.

$$Min \quad f(x,y) \tag{1}$$

$$s.t. \quad g(x,y)=0 \tag{2}$$

$$h(x,y)\le 0 \tag{3}$$

The goal of the perform $f(x,y)$ indicates the framework's efficiency target. In multi-objective OPF, f may be a scalar or matrix function. Vector variables $g(x,y)$ and $h(x,y)$ define the framework's disparity and equality requirements. The OPF problem can be turned into linear, mixed-integer, nonlinear (possibly non-convex), or mixed-integer nonlinear coding issues depending on the values of f, g and h。

A. Equation Constraints

The OPF issue involves numerous equations and inequality restrictions. The equality requirements ensure that the total power generated equals the load power plus any line losses. In contrast, inequality constraints are required for the system's safe and stable operation. The equations for both reactive and active electricity balancing are provided in polar coordinates below.

$$P_{G_i}=P_{D_i}+V_i\sum_{NB}^{j=1}V_j[G_{ij}\cos(\delta_i-\delta_j)+B_{ij}\sin(\delta_i-\delta_j),i=1,\ldots,NB \tag{4}$$

$$Q_{G_i}=Q_{D_i}+V_i\sum_{NB}^{j=1}V_j[G_{ij}\cos(\delta_i-\delta_j)+B_{ij}\sin(\delta_i-\delta_j),i=1,\ldots,NB \tag{5}$$

The active power equation constraint, represented by Eq. (4), is a fundamental component of the model, P_{D_i} denotes the active power consumption of the load, whereas P_{G_i} reflects the active power output of the i -th bus generator. Equation (5) expresses the reactive power restrictions, with Q_{D_i} signifying the load's reactive electrical consumption. And Q_{G_i} denotes reactive power output of the generator at bus i -th; δ_i denotes the phase angle of the i-th phase angle of the i-th bus; G_{ij} and B_{ij} are the i -th and j -th bus of conductance and susceptance of the transmission line between them; NB denotes the total amount of nodes. Equations (4) and (5) act as Newton-Raphson technique termination criterion. This indicates that the power flow calculation process has completed and the equation restrictions have been satisfied.

B. Inequality Constraints on Control Variables

The electric network operating state can be altered by modifying factors known as control variables or decision parameters. These include generators' active power output, voltage magnitude at generator buses, shunt capacitors' reactive power, and changeable transformer tap settings.

$$P_{G_i}^{min}\le P_{G_i}\le P_{G_i}^{max},i=1,\ldots,NG \tag{6}$$

$$V_{G_i}^{min}\le V_{G_i}\le V_{G_i}^{max},i=1,\ldots,NG \tag{7}$$

$$Q_{C_i}^{min}\le Q_{C_i}\le Q_{C_i}^{max},i=1,\ldots,NC \tag{8}$$

$$T_K^{min}\le T_K\le T_K^{max},K=1,\ldots,NT \tag{9}$$

where, Eqs. (6-7) represents generator constraints, Eq. (8) represents reactive power compensator constraints, and Eq. (9) represents transformer constraints.The complete control variables of the system can be described as follows,

$$x=[P_{G_2},\ldots,P_{G_{NG}},V_{G_1},\ldots,V_{G_{NG}},T_1,\ldots,T_{NT},\ldots,Q_{C_1},\ldots,Q_{C_{NG}}] \tag{10}$$

where, the generator's active power output is $P_{G_2},\ldots,P_{G_{NG}}$; the magnitude of the generator bus voltage is $V_{G_1},\ldots,V_{G_{NG}}$; $T_1,\ldots,T_{NT}$ is the setting of the transformer taps; $Q_{C_1},\ldots,Q_{C_{NG}}$ refers to the reactive shunt capacitor's capacity.The number of generators is denoted as NG, the number of reactive power capacitors as NC, and the number of transformers as NT.

C. Inequality Constraints on State Variables

State variables react to changes in control factors. The Newton-Raphson approach is implemented in electrical energy calculations to determine these state variables.

$$P_{Slack}^{min}\le P_{Slack}\le P_{Slack}^{max} \tag{11}$$

$$Q_{G_i}^{min} \le Q_{G_i} \le Q_{G_i}^{max}, i = 1,\ldots,NG \quad (12)$$

$$V_{L_m}^{min} \le V_{L_m} \le V_{L_m}^{max}, m = 1,\ldots,NL \quad (13)$$

$$S_{l_n} \le S_{l_n}^{max}, n = 1,\ldots,Nl \quad (14)$$

Eq. (11) is the equilibrium node constraint, Eq. (12) is the generator constraint, and Eqs. (13-14) are the safety constraints. The state variables in the system are represented as follows:

$$y = [P_{Slack_1}, V_{L_1},\ldots,V_{L_{NL}}, Q_{G_1},\ldots,Q_{G_{NG}}, S_{l_1},\ldots,S_{l_{Nl}}] \quad (15)$$

where, P_{Slack_1} indicates the active power input to the slack node, which operates in fulfilling the active power harmony criteria specified in Section 2.1. $V_{L_1},\ldots,V_{L_{NL}}$ represents the voltage across each load point. $Q_{G_1},\ldots,Q_{G_{NG}}$ represents the reactive power produced by generators, while $S_{l_1},\ldots,S_{l_{Nl}}$ represents the electric delivered via the lines. NL and Nl denotes the current load knots and the total transfer lines.

Inequality restrictions on decision variables do not require separate processing owing to their function as higher and lower limits. If the selected variable violates these boundaries, it will be adjusted to its maximum or lowest amount. Inequality requirements on state variables are controlled via penalty functions.

D. Penalty Function

In general, solving the OPF formulation becomes more computationally challenging as the system representation becomes more accurate. The presence of nonconvex objective and constraints makes the OPF problem computationally and theoretically challenging. Furthermore, complicated structural restrictions are difficult to manage using random or stochastic search methods. To solve these concerns, the penalty function method is often used. The penalty function approach converts confined OPF problems to unconstrained ones. The penalty term is stated as Eq, (16), whereas the fitting function for each scenario is recast as Eq. (17).

$$\begin{aligned} penalty = {} & K_P \times (P_{G1} - P_{G1}^{lim})^2 + K_Q \times \sum_{NG}^{i=1} (Q_{Gi} - Q_{Gi}^{lim})^2 \\ & + K_V \times \sum_{NL}^{m=1} (V_{Lm} - V_{L_m}^{lim})^2 + K_S \times \sum_{Nl}^{n=1} (S_{ln} - S_{l_n}^{lim})^2 \end{aligned} \quad (16)$$

$$fitness = f_{Casei} + penalty \quad (17)$$

where, K_P equals to the value of 10^6, K_Q equals to 10^6, K_V equals to 10^9, and K_S equals to 10^6.

III. Study Cases and Objective Functions

We exploited the standard IEEE-30 bus system to validate the proposed method's effectiveness. Table I summarizes the test system, including the placements of generators, transformers, shunt compensators, and other essential data.

Bus 1 is the swing or slack bus, also known as the $V\delta$ bus. In power flow studies, the swing bus plays a crucial role in balancing active and reactive power in a system that satisfies the power balance equation. For practical purposes, the slack bus's voltage scale and voltage angle are set to 1 p.u. and 0 degrees, respectively. The volts and angles of all other buses are normalized in relation to the swing bus and used as outputs for the load flow analysis. The following part will describe the bus test system study case's development procedure.

Fig. 1 depicts the structure of the IEEE-30 bus system, consisting of six generators, four transformers, and two electrically reactive capacitors. The active power require for the entire network is 283.4 MW, while the need for reactive electricity is 126.2 MVAR, assuming a fundamental voltage of 100 MVA. The voltage restrictions for generator buses range between 0.95 to 1.1 per unit (p.u.), while for load buses, they range from 0.95 to 1.05 p.u. Table I provides an overview of the standard IEEE-30 bus system. The examination framework encounters four unique the improvement goals: fuel cost, active power loss of the system, bus voltage variation, and constant voltage. Each goal is accomplished via single objective optimizing.

A. Case 1: Fuel Cost

This is OPF's most fundamental objective function, and it has been extensively researched in the literature. Quadratic functions are commonly used to characterize thermal generators' consumption characteristics. The objective function that must be minimized is defined as follows:

$$f_{cost} = \sum_{NG}^{i=1} a_i + b_i P_{G_i} + c_i P_{G_i}^2 \quad (18)$$

where, a_i, b_i and c_i are the cost coefficients for generating the generator's output power, while NG is the number of system units. P refers to the active output power of i-th unit. Table II illustrates the cost coefficients for generators within the IEEE-30 node the electrical network.

B. Case 2: System Active Power Loss

Eq. (19) aims to minimize the active power losses in megawatts (MW).

$$f_{Ploss} = \sum_{Nl}^{i=1} \sum_{Nl}^{j \ne i} G_{ij} [V_i^2 + V_j^2 - 2V_i V_j cos(\delta_i - \delta_j)] \quad (19)$$

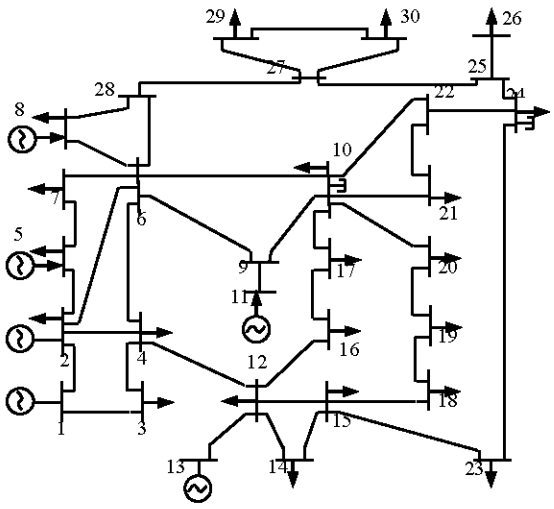

Fig. 1 Framework of standard IEEE-30 bus network

TABLE I. DETAILED DESCRIPTION OF STANDARD IEEE-30 BUS NETWORK

Item	Quantity	Details
Bus	30	-
Branch	41	-
Thermal generator	6	Buses: 1 (slack), 2, 5, 8, 11 and 13
Shunt VAR compensation	9	Buses: 10 and 24
On-load tap changer transformer	4	Branches: 11, 12,15 and 36
Control variables	17	-
Connected load	-	283.4 MW, 126.2 MVAr
Load bus voltage	24	[0.95 - 1.05] p.u.

TABLE II. GENERATOR-RELATED PARAMETERS

Generator	Bus	*a*	*b*	*c*
G_1	1	0	2	0.00375
G_2	2	0	1.75	0.0175
G_3	5	0	1	0.0625
G_4	8	0	3.25	0.00834
G_5	11	0	3	0.025
G_6	13	0	3	0.025

C. *Case 3: Voltage Stability*

Voltage stability issues have recently received more attention in the world of electrical power systems. This increased focus arises from previous occurrences in which electrical systems in specific countries failed due to voltage instability. In power systems, "stability" refers to the system's capacity to keep all bus voltages within acceptable levels after disturbances. When disturbances, increasing load demands, or changes in system circumstances result in unmanageable voltage dips, the system will unavoidably enter a state of voltage instability. Networks with longer connections and heavier loads are prone to encounter unstable voltages.

The L -index for each node provides an accurate measure of any electrical system's reliability. This index fluctuates between 0 to 1, while 0 representing empty load and scores larger than 1 indicating voltage collapse. The voltage stability metric used in this paper is obtained from a solved power flow with variables and parameters to compute the voltage stability metric, which can be used to quantitatively characterize the distance between the actual state and the stability limit. The system nodes are classified into two categories, one for all load nodes corner denoted as L, and the other for nodes including generators denoted as G. The system node equation can be expressed as:

$$\begin{bmatrix} U^L \\ U^G \end{bmatrix} = \begin{bmatrix} Y_1 & Y_2 \\ Y_3 & Y_4 \end{bmatrix} \begin{bmatrix} I_L \\ I_G \end{bmatrix} \tag{20}$$

Partial inverses are performed on it:

$$\begin{bmatrix} U^L \\ I^G \end{bmatrix} = \begin{bmatrix} H_1 & H_2 \\ H_3 & H_4 \end{bmatrix} \begin{bmatrix} I^L \\ U^G \end{bmatrix} = \begin{bmatrix} Z^{LL} & F^{LG} \\ K^{GL} & Y^{GG} \end{bmatrix} \begin{bmatrix} I^L \\ U^G \end{bmatrix} \tag{21}$$

U^G , I_G , U^L and I_L are the voltage vector and current vector of the PV node and load node; Z^{LL} , F^{LG} , K^{GL} and Y^{GG} are the submatrices of the matrix of mixtures. The local voltage stabilization index L_j is determined for each load node as follows:

$$L_j = \left| 1 - \sum_{NG}^{i=1} F_{ji} \frac{V_i}{V_j} \right| \quad j = 1, \ldots, Nl \tag{22}$$

Of these, the V_i and V_j denote the voltages of the generator of generation and the P-Q bus of the j -th generation, respectively; F_{ji} can be calculated by the YBUS matrix with the following formula:

$$F_{ji} = -[Y_{LL}]^{-1}[Y_{LG}] \tag{23}$$

where, extract submatrices Y_{LL} and Y_{LG} from the network's YBUS framework, isolating the load (PQ) and generator (PV) nodes. Calculate the L -index for all load buses; the highest number indicates reliability of the system. Hence, the ultimate operate for system security is:

$$f_{Vstability} = \max(L_j) \quad j = 1, \ldots, Nl \tag{24}$$

In the case where the generator node voltage is maintained constant, $L < 1$, with smaller values indicating a more stable system.

D. *Case 4: Voltage Stability*

Voltage deviance is an essential statistical measure used to assess the reliability of an electrical network. It indicates the condition of the system voltage. The goal function is defined as the accumulated departure of all P-Q bus voltages in the power structure, as determined using the following formula:

$$f_{Vdeviation} = \sum_{NL}^{m=1} |V_{Lm} - 1.0| \tag{25}$$

IV. NUTCRACKER OPTIMIZATION ALGORITHM

NOA is an innovative metaheuristic algorithm. The nutcracker's behavior can be categorized as two basic tasks. The first objective is to gather and store pine nuts (food). The second task comprises looking for and retrieving saved locations. These activities take place in two distinct seasons. The suggested method models the nutcracker's behavior based on these two basic actions. The two basic tactics are foraging and subsequent storage, and caching search and subsequent retrieval.In either scenario, the process of exploration and exploitation exists in the nutcracker population, i.e., each strategy in turn contains two different population behaviors, as shown in Fig. 2.

A. *Population Initialization*

The initialization of the NOA population involves randomly generating points in the problem's search space as individual nutcrackers. The formula for initialization is as follows, assuming a population size of N and problem dimension of D.

$$\vec{X}_{i,j}^{t} = + \left(\vec{U}_j - \vec{L}_j \right) \cdot \vec{RM} + \vec{L}_j, i = 1, 2, \ldots, N, j = 1, 2, \ldots, D \tag{26}$$

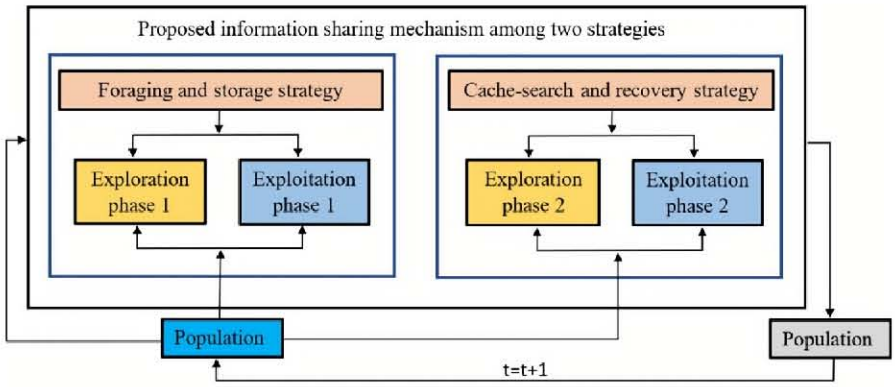

Fig. 2 Exploration and exploitation processes.

Eq. (26) denotes the j-th dimensional variable of individual i, and denotes the highest and lowest boundaries of the j-th dimensional variable, $\vec{RM}$ is an arbitrary vector between [0, 1].

B. Phase I-Exploration

As a result, the nutcracker occupies the beginning positions/food sites within the search space (gathering area) generated by Eq. (26). Subsequently, the nutcrackers assess the preliminary position of the fruit, which contains seeds. If the nutcracker comes across viable seeds, it takes them to a storage place and buries them in a cache. If suitable seeds are not found, the nutcracker looks for cones on another pine tree or several trees. The following position update method can be used to quantitatively approximate this behavior:

$$\vec{X}_i^{t+1}=\begin{cases} X_{i,j}^t, & if\ \tau_1<\tau_2 \\ X_{m,j}^t+\gamma\cdot\left(X_{A,j}^t-X_{B,j}^t\right) & \\ \quad +\mu.\left(r^2J_j-L_j\right), & if\ t\le T_{max}/2.0 \\ X_{C,j}^t+\mu\cdot\left(X_{A,j}^t-X_{B,j}^t\right) & otherwise \\ +\mu.(r_1<\delta).\left(r^2.U_j-L_j\right), & \end{cases} \quad (27)$$

where, $\vec{X}_i^{t+1}$ is the new placement of the i-th individual in the current generation; X_{ij}^t is the j-th placement of the i-th nutcracker in the present generation, L_j , U_j are scalar vectors including the lower and higher bounds of the j-th digit, ν is a real number based on Lévy's flight, and A , B and C are three persons chosen at random from the population to study the excellent state of the alimentary supply.; τ_1 , τ_2 , r , r_1 are real number generated randomly in the range of [0,1]. $X_{m,j}^t$ is the j -th dimensional mean of all solutions of the current population at the t -th iteration, t is the count of iterations, and δ is fixed to 0.05. μ is a value generated on the basis of a normal distribution (τ_4), Lévy flight (τ_4), randomly between 0 and 1 (τ_3) as follows:

$$\mu=\begin{cases}\tau_3\ if\ r_1<r_2\\ \tau_4\ if\ r_2<r_3\\ \tau_5\ if\ r_1<r_3\end{cases} \quad (28)$$

where , r_2 , r_3 are random real numbers in the range [0,1].

C. Phase I-Development

The nutcracker will initially facilitate the transfer of the food items procured during the preceding stage (Exploration Stage1) to a provisional storage location. This is the Exploitation Phase 1, which is the stage during which the nutcracker stores pine seeds. Mathematically, the behavior may be expressed as follows:

$$\vec{X}_i^{t+1(new)}=\begin{cases}\vec{X}_i^t+\mu\cdot\left(\vec{X}_{\text{best}}^t-\vec{X}_i^t\right)\cdot|\lambda|+r_1\cdot\left(\vec{X}_A^t-\vec{X}_B^t\right) & if\ \tau_1<\tau_2\\ \vec{X}_{\text{best}}^t+\mu\cdot\left(\vec{X}_A^t-\vec{X}_B^t\right) & if\ \tau_1<\tau_3\\ \vec{X}_{\text{best}}^t\cdot l & otherwise\end{cases}$$

(29)

where, $\vec{X}_i^{t+1(new)}$ is the new position of the nutcracker storage region in the present iteration t , $\vec{X}_{\text{best}}^t$ is the optimal individual of the current population, λ is a random number created by Lévy's flight, τ_3 is a number randomized from 0 to 1, and l is a decreasing linear factor from 1 to 0. In furtherance of avoiding local minima that may occur during unidirectional searches, the diversity of NOA's development operators helps to accelerate its convergence rate.

The transition between foraging and caching stages is contingent on the following equation, which strives to attain equilibrium between exploration and exploitation.

$$\vec{X}_i^{t+1}=\begin{cases}\text{Eq.(27)},\ if\ \varphi>P_{a_1}\\ \text{Eq.(29)},\ otherwise\end{cases} \quad (30)$$

where, φ is a random number ranging from 0 to 1, and P_{a_1} denotes a probability value that decreases linearly from 1 to 0 based on the present generation.

D. Cache Search and Retrieval Strategy

Throughout the winter, it is a good idea to be in exploration and search mode. The second exploration phase begins for nutcrackers as they begin to search for their cache. Nutcrackers use spatial tactics to locate their caches, typically using multiple reference points to cue a hiding place. For simplicity, let us assume that every cache is identified by two objects, called reference points (RP). The two chosen landmarks are computed as follows:

$$\overrightarrow{RP}_{i,1}^{t}=\begin{cases}\vec{X}_i^t+\alpha\cdot\cos(\theta)\cdot\left(\left(\vec{X}_A^t-\vec{X}_B^t\right)\right)+\alpha\cdot RP, & if\ \theta=\pi/2\\ \vec{X}_i^t+\alpha\cdot\cos(\theta)\cdot\left(\left(\vec{X}_A^t-\vec{X}_B^t\right)\right), & \text{otherwise}\end{cases} \tag{31}$$

$$\overrightarrow{RP}_{i,2}^{t}=\begin{cases}\vec{X}_i^t+\left(\alpha\cdot\cos(\theta)\cdot\left(\left(\vec{U}-\vec{L}\right)\cdot\tau_3+\vec{L}\right)+\alpha\cdot \mathrm{RP}\right)\cdot\vec{U}_2, & \text{if}\theta=\pi/2\\ \vec{X}_i^t+\alpha\cdot\cos(\theta)\cdot\left(\left(\vec{U}-\vec{L}\right)\cdot\tau_3+\vec{L}\right)\cdot\vec{U}_2, & \text{otherwise}\end{cases} \tag{32}$$

$$\overrightarrow{U_1}=\begin{cases}1 & \vec{r_2}<P_{rp}\\ 0 & \text{otherwise}\end{cases} \tag{33}$$

$$\alpha=\begin{cases}\left(1-\dfrac{t}{T_{max}}\right)^{2\frac{t}{T_{max}}}, & if\ r_1>r_2\\ \left(\dfrac{t}{T_{max}}\right)^{\frac{2}{t}}, & otherwise\end{cases} \tag{34}$$

where, θ is a random radian between $[0,\pi]$. A, B are two different individual nutcrackers randomly selected. r and r_2 are random real numbers in the range $[0,1]$. T is the maximum number of iterations, and the very first reference point is generated by using Eq. (33). P_{rp} is the probability used to determine the percentage of the search space that is used to explore the rest of the regions globally, where t and T_{max} rand display the present and maximal generation, correspondingly. The first term in Eq. (34) reduces exponentially with the number of iterations, which improves the algorithm's convergence rate. Simultaneously, the second term grows gradually to avoid becoming trapped in local minima. .

E. Phase II-Exploration

There are several possibilities for a nutcracker to locate its cache of food.The first hypothesis is that the nutcracker remembers the position of its cache using the first RP value. The second option is that the nutcracker can't remember where its cache is.In this case it will search using the second RP , which is the second stage of development shown in Eq. (38). For the first case location, there are two possibilities: Either the food exists or it does not. The following equation can be used to mathematically model this behavior:

$$X_{i,j}^{t+1}=\begin{cases}X_{i,j}^{t}, & if\ \tau_3<\tau_4\\ X_{i,j}^{t}+r_1\cdot\left(X_{best,j}^{t}-X_{i,j}^{t}\right)+\mathrm{r}_2\cdot\left(\overrightarrow{RP_{i,1}^{t}}-X_{C,j}^{t}\right), & otherwise\end{cases} \tag{35}$$

Eq. (35) has two states. The first state models the possibility that food exists, which means that certain dimensions of the cache/solution have a probability of surviving the next generation. It is beneficial to keep a stock of pine nuts. Indeed, the nutcracker will put emphasis on food storage the following time. The second situation of Eq. (35) represents the risk of no food being available.

Due to poor solution spaces, the algorithm uses an escape strategy to prevent slipping to the minima. Hidden things may be stolen by other nutcrackers and lost, or it may be damaged by natural forces such as rain or snow. Eq. (35) and state (1) enable the nutcracker to investigate potential portions of the search space, improving NOA's local search capabilities. Eq. (35) and state (2) allow the nutcracker to explore places in the search space, enhancing NOA's global search capabilities.

$$X_{i,j}^{t+1}=\begin{cases}X_{i,j}^{t}, & if\ \tau_5<\tau_6\\ X_{i,j}^{t}+r_1\cdot\left(X_{best,j}^{t}-X_{i,j}^{t}\right)+\mathrm{r}_2\cdot\left(\overrightarrow{RP_{i,2}^{t}}-X_{C,j}^{t}\right), & otherwise\end{cases} \tag{36}$$

where, $RP_{i,2}^{t}$ is the second RP of the i -th nutcracker's current cache at iteration t . Using Eq. (39), the Nutcracker Optimization Algorithm (NOA) can investigate new ranges surrounding the second reference point (RP) and develop viable ranges for possible solutions. NOA implies each nutcracker utilizes the second RP to locate the stash, and therefore, Eq. (35) is updated to Eq. (36) based on the second RP .The first stage of Eq (35) permits the algorithm to focus its search on the most suitable region containing the best solution. Using the second state of Eq. (36), the method can explore new parts of the search space and improve its overall search. In conclusion, the simulation of retrieval behavior can be summarized as follows:

$$\vec{X}_i^{t+1}=\begin{cases}\text{Eq.(34)}, if\ \tau_7<\tau_8\\ \text{Eq.(35)}, otherwise\end{cases} \tag{37}$$

where, τ_7 and τ_8 are random numbers between the range [0, 1]. The 1st example in the formula represents the nutcracker that remembers its hidden cache, while the 2nd example represents the nutcracker that does not remember.

F. Phase II-Development

Eqs. (38)-(39) depict the second stage of development.

$$\vec{X}_i^{t+1}=\begin{cases}\vec{X}_i^t, if\ f(\vec{X}_i^t)<f(\overrightarrow{RP}_{i,1}^t)\\ \overrightarrow{RP}_{i,1}^t, otherwise\end{cases} \tag{38}$$

$$\vec{X}_i^{t+1}=\begin{cases}\vec{X}_i^t, if\ f(\vec{X}_i^t)<f(\overrightarrow{RP}_{i,2}^t)\\ \overrightarrow{RP}_{i,2}^t, otherwise\end{cases} \tag{39}$$

The equation determines the trade-off between exploratory behavior for the first and second RP .

$$\vec{X}_i^{t+1}=\begin{cases}\text{Eq.(38)}, if\ f(\text{Eq.(38)})<f(\text{Eq.(39)})\\ \text{Eq.(38)}, otherwise\end{cases} \tag{40}$$

The subsequent formula determines the interchange during cache search cycles and the retrieval phase in order to strike an equilibrium between exploration and exploitation.

$$\vec{X}_i^{t+1}=\begin{cases}\text{Eq.(37)}, if\ \phi>P_{a_2}\\ \text{Eq.(40)}, \text{otherwise}\end{cases} \tag{41}$$

Update the optimal value by Eq. (42).

$$\vec{X}_i^{t+1} = \begin{cases} \vec{X}_i^{t+1}, & if\ f(\vec{X}_i^{t+1}) < f(\vec{X}_i^{t}) \\ \vec{X}_i^{t}, & otherwise \end{cases} \quad (42)$$

The procedure of the Nutcracker Optimization Algorithm is depicted in Fig. 3.

V. Function Optimization Simulation and Result Analysis

A. Test Function

To evaluate the efficiency of the Nutcracker optimization algorithm, this section employs the CEC2017 benchmark functions, consisting of 29 functions for testing single-peak, multimodal, hybrid, and combinatorial problems with shifts and rotations. It is important to note that the F2 functions have unresolved issues that are not considered[23]. The search domain for all functions is [-100, 100], and their dimension is 10. This section compares seven algorithms: Nutcracker Optimization Algorithm (NOA), Harris Hawk Optimization Algorithm (HHO), Sandy Cat Swarm Optimization Algorithm (SCSO), Gray Wolf Optimizer (GWO), Whale Optimization Algorithm (WOA), Beluga Whale Optimizer (BWO), and Dung Beetle Optimization Algorithm (DBO). Each algorithm was tested with 50 populations, 500 iterations, and 30 independent runs of each test function. The results were plotted against their averages.

B. Simulation Results and Analysis

Table III and Fig. 4 show that the NOA performs well in all types of benchmark functions. For the single-peak functions (F1, F3), the performance is ranked first for all of them. In the simple multi-peak functions (F4-F10), F4 and F10 have the best performance. In the hybrid functions (F11-F20), F11-F15, F18 and F19 have the best performance. In the combined functions (F21-F30), F25, F27, F28 and F30 rank first in terms of performance. According to the comprehensive performance analysis, NOA ranks first on average among 29 tested functions, followed by DBO in second place. The BWO ranks the lowest. Effectiveness of Nutcracker optimization algorithm has been proven.

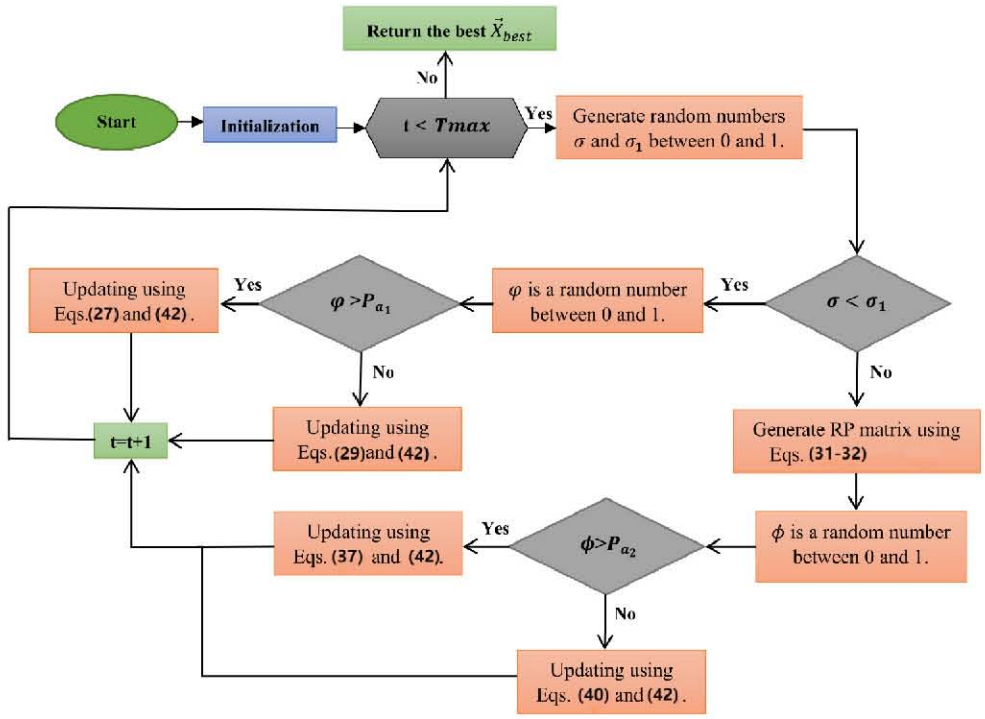

Fig. 3 NOA flow chart.

TABLE III. CEC2017 BENCHMARK FUNCTION SIMULATION RESULTS

		NOA	HHO	SCSO	GWO	WOA	BWO	DBO
F1	MINIMUM	2.28E+05	2.00E+07	1.32E+09	1.46E+08	1.58E+09	4.22E+10	1.69E+05
	MAXIMUM	3.62E+06	5.66E+07	1.84E+10	6.33E+09	2.17E+10	7.48E+10	4.33E+06
	AVERAGE	1.23E+06	3.88E+07	8.72E+09	1.75E+09	1.02E+10	6.55E+10	1.34E+06
	RANK	1	3	5	4	6	7	2
F3	MINIMUM	7.17E+03	2.84E+04	3.42E+04	3.86E+04	1.69E+04	7.93E+04	3.72E+04
	MAXIMUM	3.74E+04	6.44E+04	8.53E+04	1.19E+05	5.42E+04	1.11E+05	8.24E+04
	AVERAGE	1.81E+04	4.60E+04	5.94E+04	7.17E+04	3.82E+04	9.25E+04	6.30E+04
	RANK	1	3	4	6	2	7	5
F4	MINIMUM	4.40E+02	5.23E+02	7.17E+02	5.25E+02	5.91E+02	1.25E+04	4.67E+02
	MAXIMUM	2.24E+02	6.90E+02	4.16E+03	7.03E+02	1.84E+03	2.16E+04	5.48E+02
	AVERAGE	5.08E+02	5.89E+02	1.59E+03	5.91E+02	9.27E+02	1.71E+04	5.10E+02

	RANK	1	3	6	4	5	7	2
	MINIMUM	5.96E+02	6.76E+02	7.00E+02	5.75E+02	6.69E+02	8.92E+02	6.36E+02
F5	MAXIMUM	3.03E+02	8.31E+02	8.73E+02	7.56E+02	8.59E+02	9.74E+02	7.91E+02
	AVERAGE	6.99E+02	7.51E+02	7.95E+02	6.33E+02	7.58E+02	9.48E+02	7.37E+02
	RANK	2	4	6	1	5	7	3
	MINIMUM	6.16E+02	6.46E+02	6.49E+02	6.03E+02	6.51E+02	6.82E+02	6.05E+02
F6	MAXIMUM	4.76E+01	6.82E+02	6.81E+02	6.23E+02	6.86E+02	7.01E+02	6.27E+02
	AVERAGE	6.30E+02	6.66E+02	6.65E+02	6.09E+02	6.65E+02	6.93E+02	6.13E+02
	RANK	3	6	5	1	4	7	2
	MINIMUM	8.31E+02	1.10E+03	1.04E+03	8.31E+02	1.00E+03	1.38E+03	9.31E+02
F7	MAXIMUM	3.23E+02	1.37E+03	1.40E+03	1.00E+03	1.37E+03	1.52E+03	1.08E+03
	AVERAGE	9.33E+02	1.23E+03	1.25E+03	9.18E+02	1.17E+03	1.47E+03	9.92E+02
	RANK	2	5	6	1	4	7	3
	MINIMUM	9.21E+02	9.19E+02	9.30E+02	8.57E+02	9.38E+02	1.11E+03	8.98E+02
F8	MAXIMUM	2.40E+02	1.03E+03	1.12E+03	1.06E+03	1.07E+03	1.18E+03	1.05E+03
	AVERAGE	9.74E+02	9.73E+02	1.01E+03	9.17E+02	1.00E+03	1.15E+03	9.90E+02
	RANK	3	2	6	1	5	7	4
	MINIMUM	1.41E+03	4.12E+03	3.33E+03	1.11E+03	3.72E+03	8.66E+03	1.35E+03
F9	MAXIMUM	6.73E+03	1.10E+04	9.05E+03	4.92E+03	1.05E+04	1.22E+04	1.06E+04
	AVERAGE	4.16E+03	7.69E+03	6.65E+03	2.26E+03	6.77E+03	1.12E+04	5.08E+03
	RANK	2	6	4	1	5	7	3
	MINIMUM	3.83E+03	4.18E+03	4.74E+03	3.30E+03	4.56E+03	7.61E+03	6.17E+03
F10	MAXIMUM	6.49E+03	7.59E+03	8.94E+03	9.49E+03	7.95E+03	9.21E+03	8.68E+03
	AVERAGE	5.08E+03	5.96E+03	6.32E+03	6.30E+03	6.10E+03	8.59E+03	7.87E+03
	RANK	1	2	5	4	3	7	6
	MINIMUM	1.16E+03	1.22E+03	1.50E+03	1.23E+03	1.35E+03	4.65E+03	1.33E+03
F11	MAXIMUM	3.08E+02	1.62E+03	6.08E+03	4.53E+03	4.07E+03	4.43E+04	1.71E+03
	AVERAGE	1.28E+03	1.36E+03	3.01E+03	2.06E+03	1.85E+03	1.77E+04	1.48E+03
	RANK	1	2	6	5	4	7	3
	MINIMUM	7.66E+04	1.57E+06	2.08E+07	2.18E+06	1.49E+07	1.14E+10	3.94E+05
F12	MAXIMUM	3.72E+06	1.82E+08	3.34E+09	2.40E+08	7.29E+08	2.11E+10	1.15E+07
	AVERAGE	8.29E+05	3.18E+07	6.30E+08	6.69E+07	2.39E+08	1.67E+10	2.47E+06
	RANK	1	3	6	4	5	7	2
	MINIMUM	2.20E+03	1.28E+05	2.62E+04	3.29E+04	3.01E+04	2.20E+09	6.39E+03
F13	MAXIMUM	6.13E+04	6.16E+06	6.56E+08	7.75E+07	9.60E+06	2.26E+10	4.48E+06
	AVERAGE	1.66E+04	9.32E+05	4.80E+07	6.59E+06	1.07E+06	1.22E+10	4.89E+05
	RANK	1	3	6	5	4	7	2
	MINIMUM	1.47E+03	8.02E+04	6.42E+04	3.74E+03	1.73E+03	2.84E+06	2.07E+04
F14	MAXIMUM	9.39E+02	3.84E+06	3.50E+06	2.89E+06	1.50E+05	6.12E+07	1.63E+06
	AVERAGE	1.62E+03	9.12E+05	8.52E+05	4.74E+05	4.08E+04	1.62E+07	1.75E+05
	RANK	1	6	5	4	2	7	3
	MINIMUM	1.64E+03	2.29E+04	1.82E+04	3.39E+04	8.46E+03	1.75E+08	2.47E+03
F15	MAXIMUM	4.01E+04	3.24E+05	7.78E+07	6.88E+06	1.95E+05	2.47E+09	6.15E+04
	AVERAGE	5.93E+03	1.24E+05	4.06E+06	1.44E+06	5.54E+04	1.13E+09	1.47E+04
	RANK	1	4	6	5	3	7	2
	MINIMUM	1.99E+03	2.21E+03	2.79E+03	2.11E+03	2.54E+03	4.20E+03	2.22E+03
F16	MAXIMUM	1.98E+03	4.36E+03	6.25E+03	3.67E+03	4.21E+03	1.08E+04	3.91E+03
	AVERAGE	2.83E+03	3.17E+03	3.73E+03	2.67E+03	3.40E+03	7.75E+03	3.03E+03
	RANK	2	4	6	1	5	7	3
	MINIMUM	2.04E+03	2.19E+03	2.01E+03	1.77E+03	1.97E+03	3.09E+03	1.86E+03
F17	MAXIMUM	1.06E+03	3.10E+03	2.99E+03	2.58E+03	2.84E+03	1.48E+04	2.75E+03
	AVERAGE	2.40E+03	2.69E+03	2.54E+03	2.12E+03	2.45E+03	5.71E+03	2.33E+03
	RANK	3	6	5	1	4	7	2

	MINIMUM	8.92E+03	2.07E+05	6.04E+04	9.00E+04	4.55E+04	2.04E+07	1.15E+05
F18	MAXIMUM	3.73E+05	1.11E+07	1.81E+07	1.12E+07	1.23E+06	4.86E+08	3.62E+06
	AVERAGE	3.73E+04	2.80E+06	2.64E+06	2.60E+06	3.22E+05	1.94E+08	1.38E+06
	RANK	1	6	5	4	2	7	3
	MINIMUM	1.95E+03	2.74E+04	2.80E+05	4.94E+03	3.34E+04	1.48E+08	2.24E+03
F19	MAXIMUM	2.82E+04	6.06E+06	3.17E+08	4.52E+07	2.02E+06	2.49E+09	3.89E+05
	AVERAGE	7.53E+03	1.59E+06	1.45E+07	3.80E+06	5.90E+05	1.19E+09	2.99E+04
	RANK	1	4	6	5	3	7	2
	MINIMUM	2.13E+03	2.37E+03	2.40E+03	2.13E+03	2.31E+03	2.77E+03	2.13E+03
F20	MAXIMUM	1.12E+03	3.26E+03	3.17E+03	2.93E+03	3.19E+03	3.12E+03	2.86E+03
	AVERAGE	2.59E+03	2.80E+03	2.75E+03	2.44E+03	2.73E+03	2.96E+03	2.60E+03
	RANK	2	6	5	1	4	7	3
	MINIMUM	2.43E+03	2.41E+03	2.47E+03	2.36E+03	2.46E+03	2.61E+03	2.42E+03
F21	MAXIMUM	5.21E+02	2.66E+03	2.65E+03	2.53E+03	2.65E+03	2.86E+03	2.57E+03
	AVERAGE	2.50E+03	2.55E+03	2.56E+03	2.41E+03	2.54E+03	2.73E+03	2.51E+03
	RANK	2	5	6	1	4	7	3
	MINIMUM	2.31E+03	2.33E+03	3.15E+03	2.43E+03	2.72E+03	6.75E+03	2.31E+03
F22	MAXIMUM	5.96E+03	9.09E+03	9.62E+03	1.05E+04	9.83E+03	1.06E+04	2.37E+03
	AVERAGE	5.94E+03	4.16E+03	6.89E+03	5.40E+03	6.88E+03	9.37E+03	2.32E+03
	RANK	4	2	6	3	5	7	1
	MINIMUM	2.73E+03	2.83E+03	2.88E+03	2.69E+03	2.85E+03	3.50E+03	2.71E+03
F23	MAXIMUM	8.42E+02	3.22E+03	3.26E+03	2.93E+03	3.16E+03	4.26E+03	2.91E+03
	AVERAGE	2.91E+03	2.99E+03	3.04E+03	2.80E+03	3.03E+03	3.86E+03	2.83E+03
	RANK	3	4	6	1	5	7	2
	MINIMUM	2.95E+03	2.92E+03	2.93E+03	2.87E+03	3.01E+03	3.54E+03	2.93E+03
F24	MAXIMUM	1.09E+03	3.30E+03	3.45E+03	3.09E+03	3.31E+03	4.88E+03	3.10E+03
	AVERAGE	3.19E+03	3.09E+03	3.16E+03	2.96E+03	3.17E+03	4.14E+03	3.02E+03
	RANK	6	3	4	1	5	7	2
	MINIMUM	2.88E+03	2.92E+03	3.00E+03	2.92E+03	3.01E+03	4.75E+03	2.89E+03
F25	MAXIMUM	4.42E+02	3.06E+03	3.72E+03	3.07E+03	3.66E+03	6.55E+03	2.94E+03
	AVERAGE	2.90E+03	2.98E+03	3.21E+03	2.99E+03	3.18E+03	5.68E+03	2.90E+03
	RANK	1	3	6	4	5	7	2
	MINIMUM	2.83E+03	2.94E+03	5.96E+03	3.66E+03	4.63E+03	9.93E+03	2.84E+03
F26	MAXIMUM	5.04E+03	9.18E+03	9.03E+03	6.37E+03	1.06E+04	1.44E+04	7.33E+03
	AVERAGE	5.77E+03	7.25E+03	7.75E+03	5.14E+03	7.60E+03	1.25E+04	4.65E+03
	RANK	3	4	6	2	5	7	1
	MINIMUM	3.22E+03	3.26E+03	3.32E+03	3.22E+03	3.28E+03	3.96E+03	3.20E+03
F27	MAXIMUM	8.67E+02	3.64E+03	3.86E+03	3.30E+03	3.69E+03	5.20E+03	3.37E+03
	AVERAGE	3.25E+03	3.36E+03	3.52E+03	3.26E+03	3.42E+03	4.70E+03	3.26E+03
	RANK	1	4	6	2	5	7	3
	MINIMUM	3.21E+03	3.27E+03	3.44E+03	3.31E+03	3.40E+03	7.18E+03	3.21E+03
F28	MAXIMUM	5.10E+02	3.52E+03	4.99E+03	3.57E+03	4.75E+03	8.87E+03	3.31E+03
	AVERAGE	3.24E+03	3.34E+03	3.86E+03	3.43E+03	3.72E+03	8.24E+03	3.26E+03
	RANK	1	3	6	4	5	7	2
	MINIMUM	3.55E+03	4.16E+03	4.34E+03	3.68E+03	3.73E+03	6.43E+03	3.53E+03
F29	MAXIMUM	1.65E+03	5.93E+03	6.01E+03	4.70E+03	5.74E+03	2.97E+04	4.72E+03
	AVERAGE	4.09E+03	4.77E+03	5.00E+03	3.98E+03	4.82E+03	1.27E+04	3.98E+03
	RANK	3	4.00E+00	6.00E+00	1.00E+00	5.00E+00	7.00E+00	2.00E+00
	MINIMUM	7.13E+03	7.29E+05	7.05E+05	4.76E+05	4.76E+05	3.73E+08	1.20E+04
F30	MAXIMUM	4.72E+04	1.89E+07	5.56E+07	3.83E+07	2.67E+07	6.24E+09	9.17E+06
	AVERAGE	2.00E+04	6.40E+06	1.74E+07	1.19E+07	6.67E+06	2.26E+09	6.25E+05
	RANK	1	3	6	5	4	7	2
	AVERAGE RANK	1.90	3.90	5.55	2.86	4.24	7.00	2.59

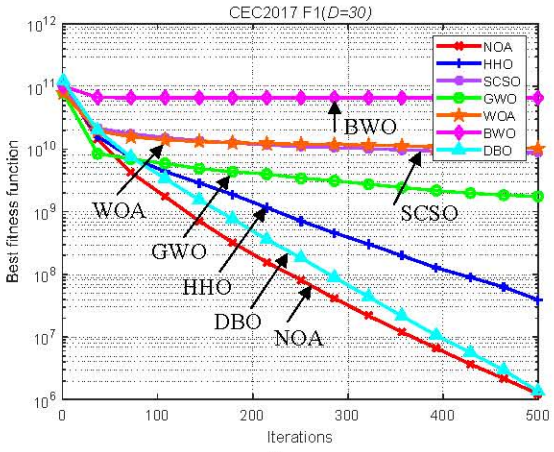

(a) F1

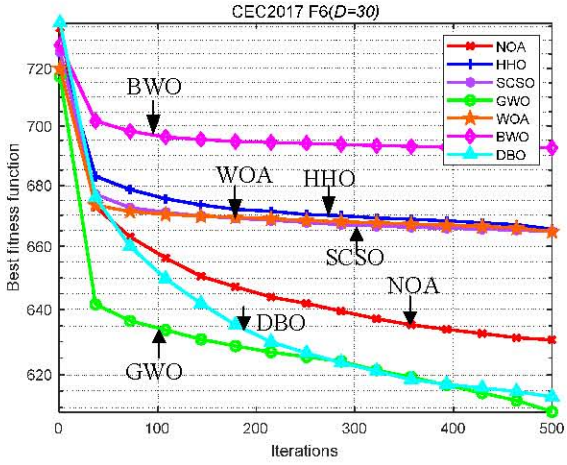

(e) F6

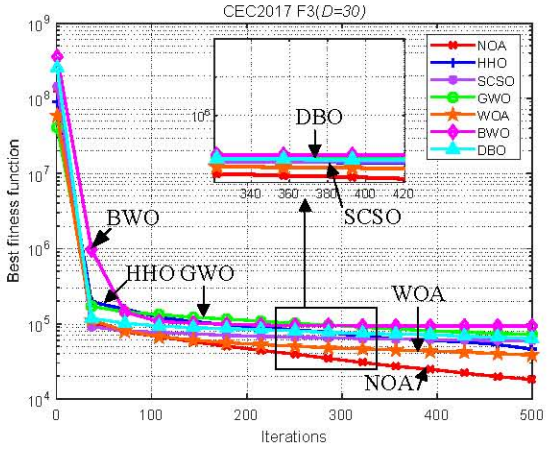

(b) F3

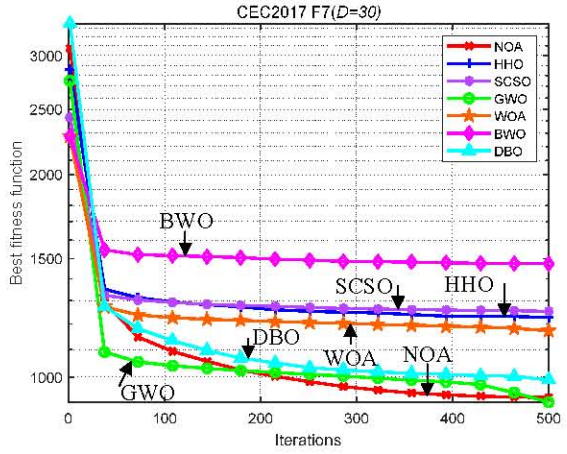

(f) F7

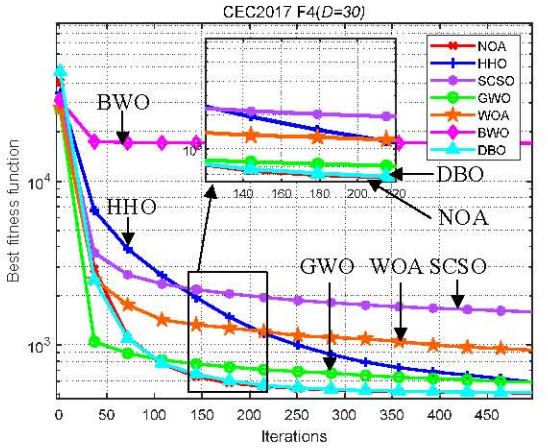

(c) F4

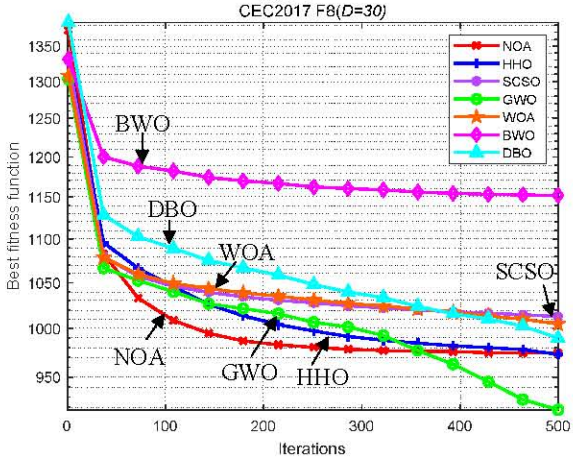

(g) F8

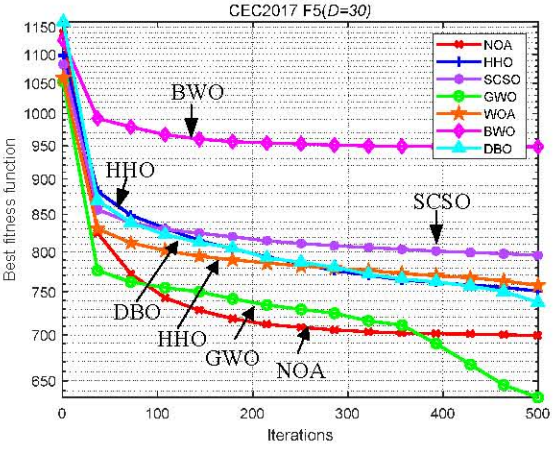

(d) F5

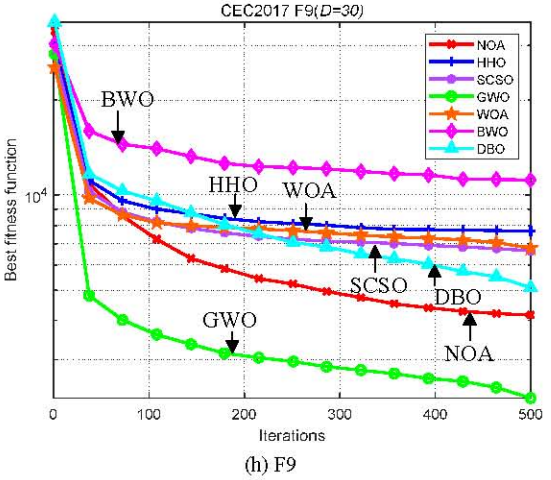

(h) F9

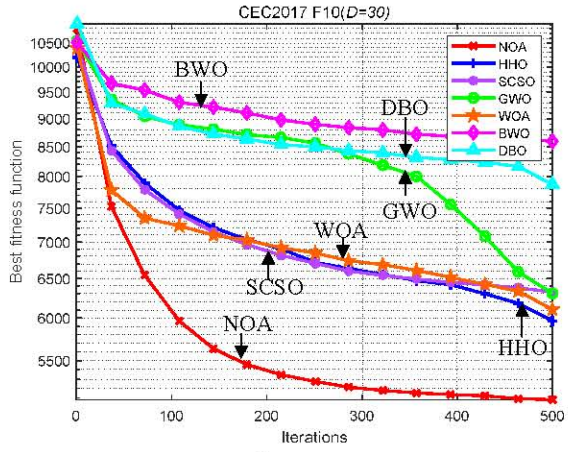

(i) F10

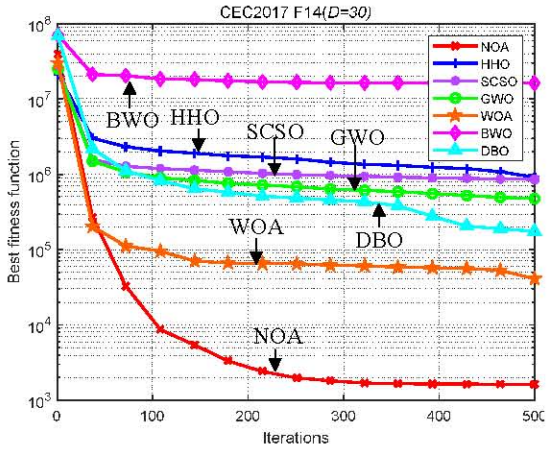

(m) F14

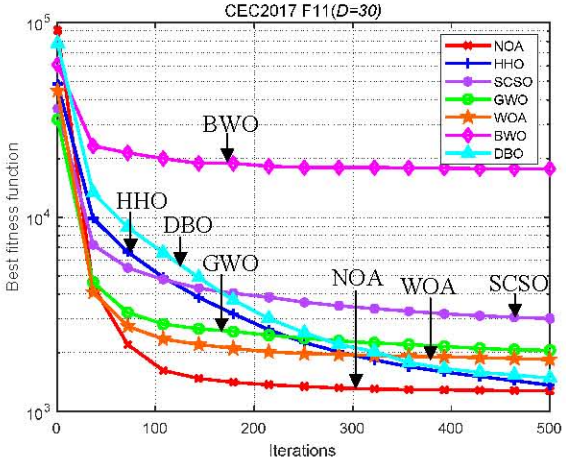

(j) 11

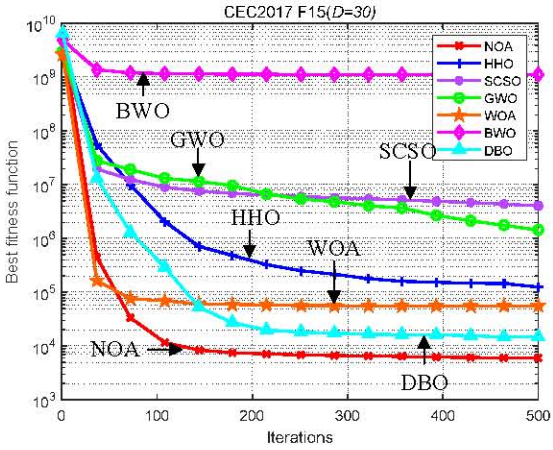

(n) F15

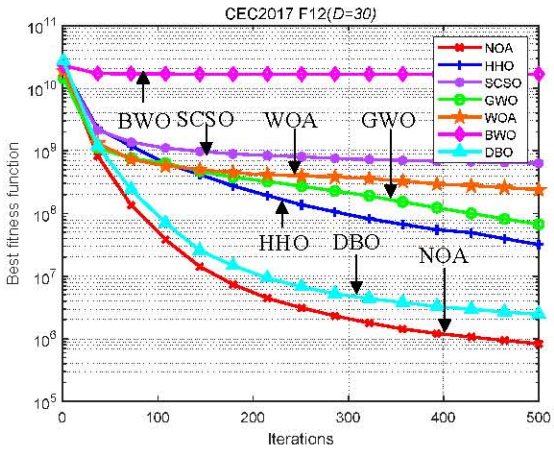

(k) F12

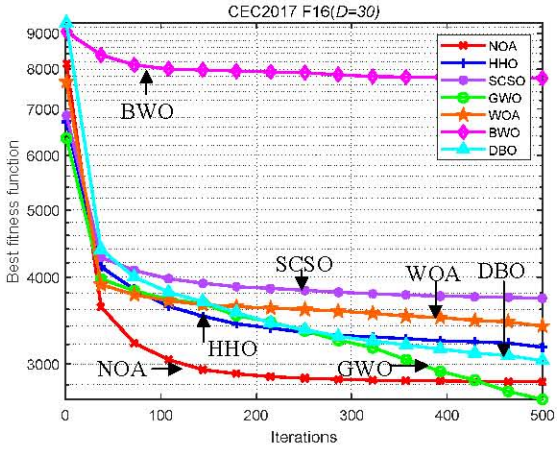

(o) F16

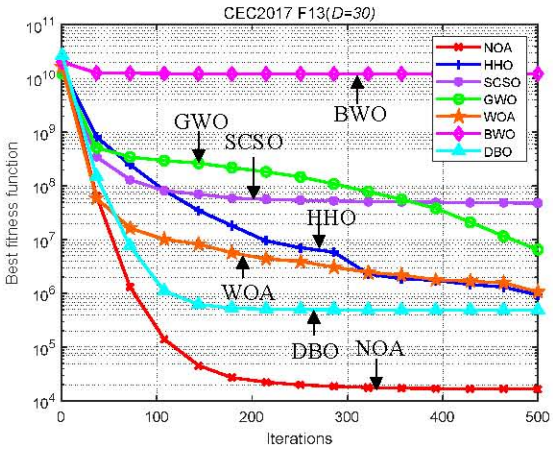

(l) F13

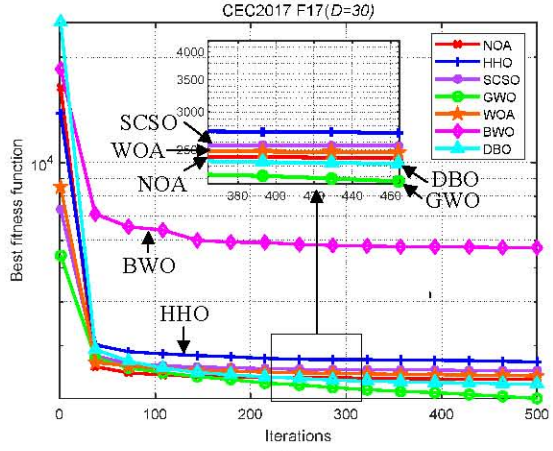

(p) F17

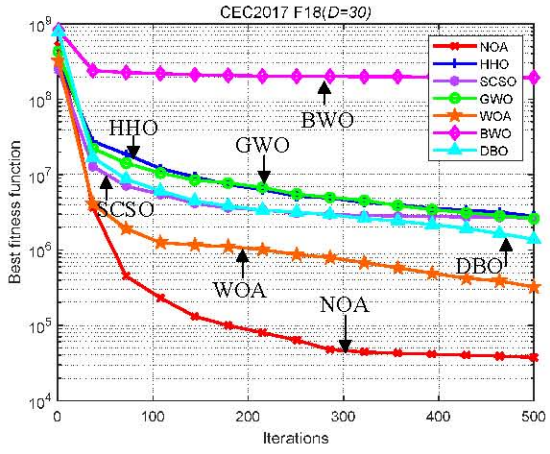

(q) F18

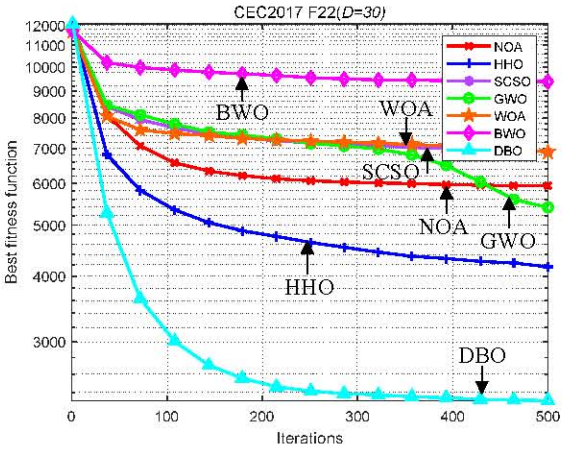

(u) F22

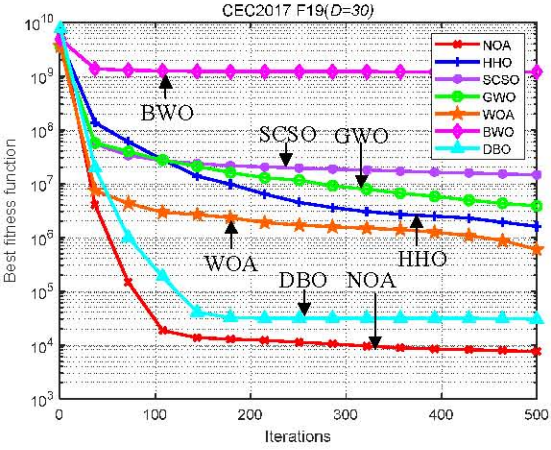

(r) F19

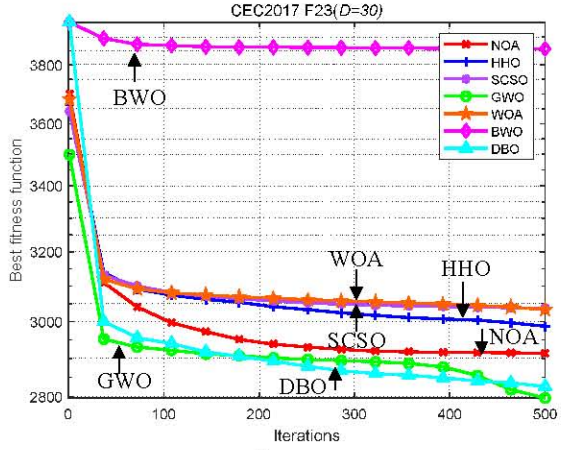

(v) F23

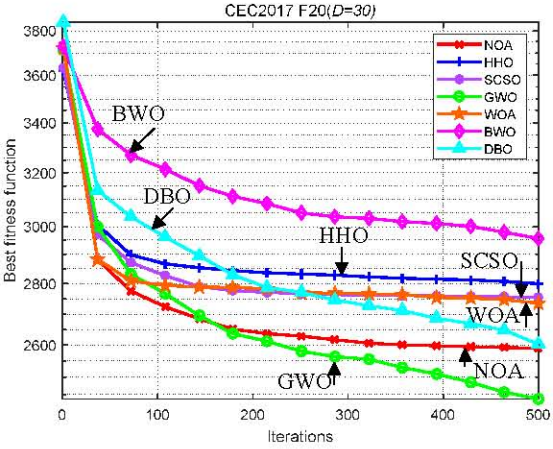

(s) F20

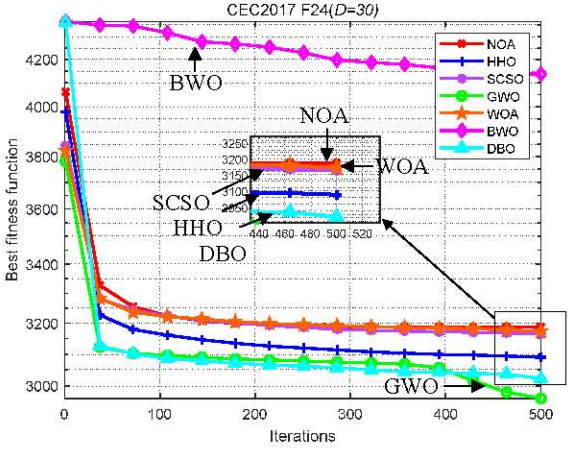

(w) F24

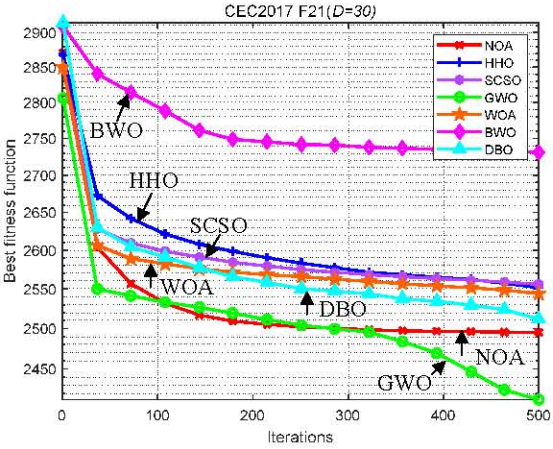

(t) F21

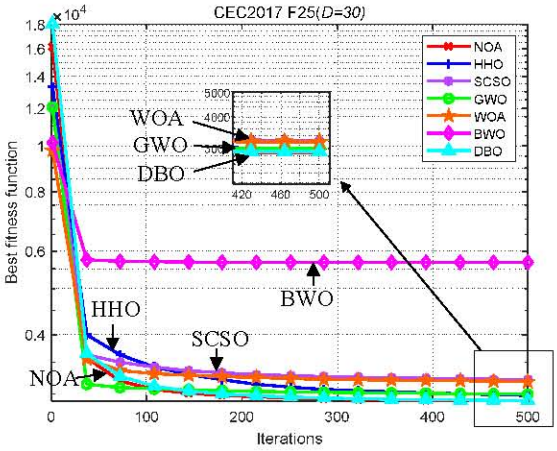

(x) F25

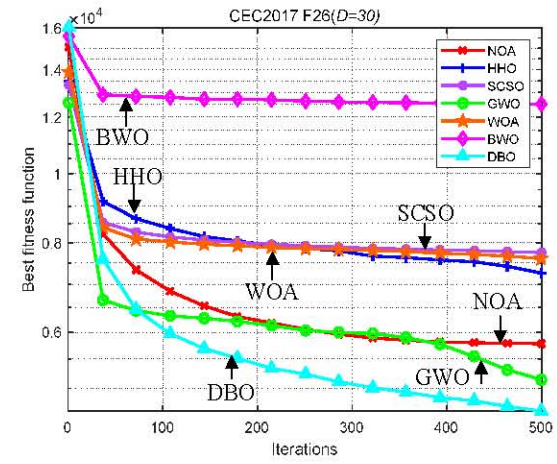

(y) F26

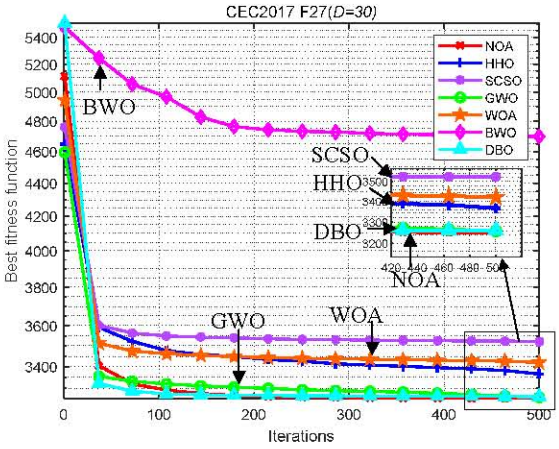

(z) F27

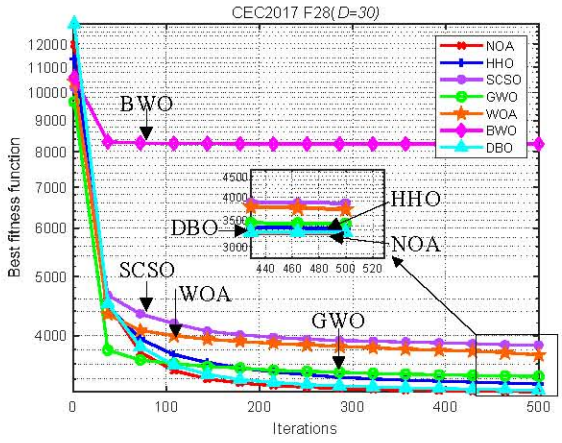

(aa) F28

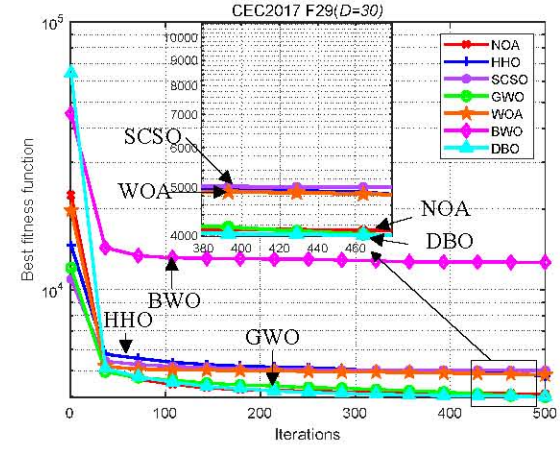

(ab) F29

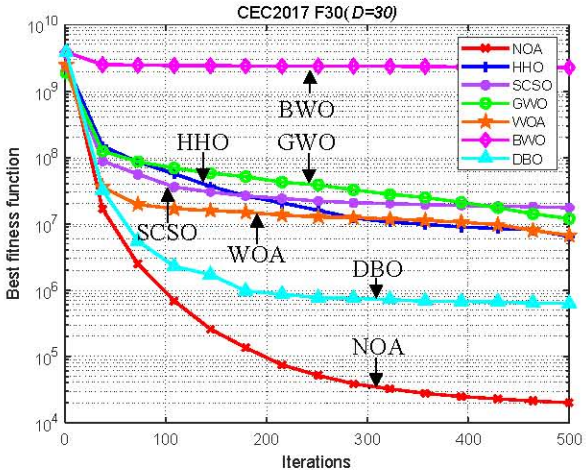

(ac) F30

Fig. 4 Convergence plot of test function optimization.

VI. Solving Optimal Power Flow Calculation Based on Nutcracker Optimization Algorithm

The nutcracker optimization approach was evaluated in an IEEE-30 bus system with a population size of 50, up to 100 iterations, and 30 independent runs per objective function. This methodology allows for thorough assessment of the algorithm's performance across objective functions.

A. Results of Case 1

The objective of optimization is to minimize power generation costs, with lower values indicating greater cost savings. Figure 5 depicts the iteration curves for each algorithm in Case 1, with the mean of 30 iterations plotted. Table IV quantitatively contrasts the execution performance for goal condition 1, illustrating the minimal, mean, and maximal costs achieved using the Nutcracker Optimization Algorithm (NOA) and other algorithms. The NOA achieved a minimum cost of $799.2885/h and the lowest average cost of $799.6691/h, demonstrating high stability. Table V shows the ideal response values for every purpose of the IEEE 30 node grid, with Scenario 1 indicating the optimal objective.

B. Outcomes of Case 2

The objective function is active power loss, where a smaller value indicates lower power transmission losses and higher active power delivered to each load. Figure 6 illustrates the iteration curve of the algorithm in Case 2. Tables VI and VII present comparative results with other algorithms in the selected test system, showing an average improvement of 8.98% compared to the second-ranked DBO.

C. Results of Case 3

The objective function is voltage stability, with a smaller value suggesting greater reliability of voltage in the electrical network. Figure 7 depicts the iteration bends for each algorithm. Table VIII presents a statistical assessment of the computational outcomes for the specified test system's objective features. NOA achieves the lowest average value at 0.7939 p.u.Table IX shows the optimal solution of NOA compared to the other algorithms, with an improvement of 0.12% compared to the second-place mean value of DBO.

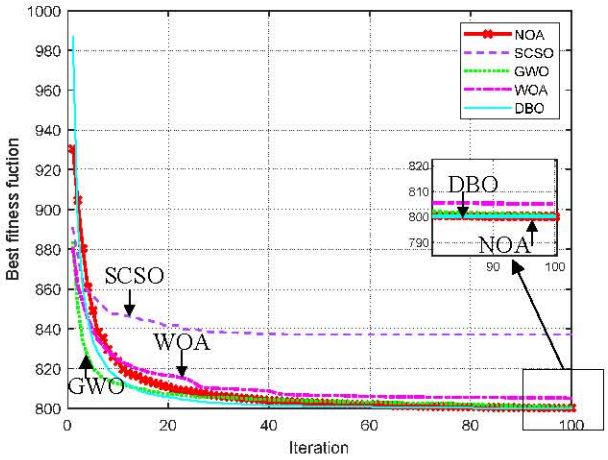

Fig. 5 Iteration curves for each algorithm in Case 1.

TABLE IV. OUTCOMES OF EACH ALGORITHM IN CASE 1

Algorithm	Minimum	Maximum	Mean
NOA	799.2885	800.7	799.6691
SCSO	819.8739	887	844.1057
GWO	799.6103	803.3	800.7068
WOA	799.9401	826.9	805.1256
DBO	799.2204	801.4	799.9427

TABLE V. COMPARISON OF EACH OBJECTIVE FUNCTION WITH CASE 1 AS THE OPTIMAL OBJECTIVE AND OTHER ALGORITHMS

Algorithm	Fuel cost	Ploss	LKmax	VD
NOA	799.2885	8.7768	0.9843	2.0589
SCSO	819.8739	10.3343	0.9954	0.8507
GWO	799.6103	8.9354	0.9809	1.6098
WOA	799.9401	9.0045	0.9843	2.2950
DBO	799.2204	8.7311	0.9812	2.1176

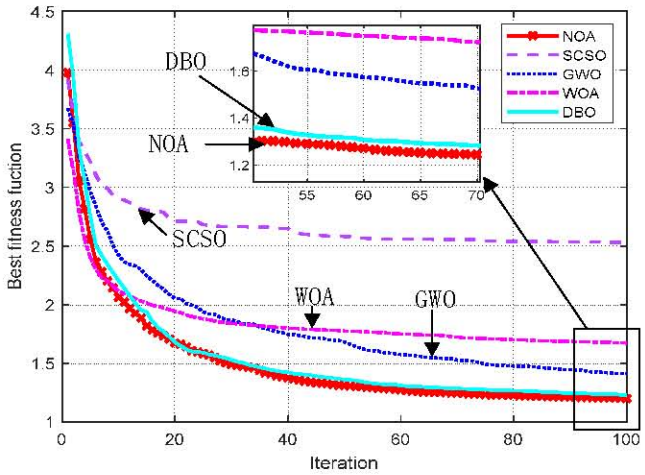

Fig. 6 Iteration bights of each algorithm in Case 2.

TABLE VI. RESULTS OF EACH ALGORITHM IN CASE 2

Algorithm	Minimum	Maximum	Mean
NOA	1.1516	1.2757	1.1990
SCSO	1.5408	3.7978	2.5299
GWO	1.1999	1.7372	1.4101
WOA	1.2931	2.839	1.6708
DBO	1.1511	1.3793	1.2294

TABLE VII. COMPARISON OF EACH OBJECTIVE FUNCTION WITH CASE 2 AS THE OPTIMAL OBJECTIVE AND OTHER ALGORITHMS

Algorithm	Fuel cost	Ploss	LKmax	VD
NOA	1485.6818	1.1516	0.9825	2.7065
SCSO	1775.7661	1.5408	0.9899	2.4481
GWO	1508.4712	1.1999	0.9835	2.4374
WOA	1475.7729	1.2931	0.9824	2.5638
DBO	1438.2398	1.1511	0.9835	2.6344

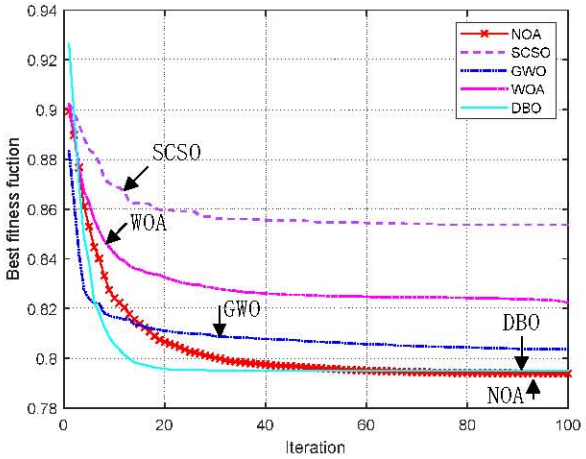

Fig. 7 Iteration bights of each algorithm in Case 3.

TABLE VIII. RESULTS OF EACH ALGORITHM IN CASE 3

Algorithm	Minimum	Maximum	Mean
NOA	0.7934	0.7957	0.7939
SCSO	0.8179	0.9237	0.8537
GWO	0.7955	0.8136	0.8036
WOA	0.7995	0.8735	0.8225
DBO	0.7935	0.8071	0.7949

TABLE IX. COMPARISON OF EACH OBJECTIVE FUNCTION WITH CASE 3 AS THE OPTIMAL OBJECTIVE AND OTHER ALGORITHMS

Algorithm	Fuel cost	Ploss	LKmax	VD
NOA	1313.8565	22.1283	0.7934	1.1244
SCSO	1777.3322	20.2741	0.8179	0.9605
GWO	1231.1344	20.7093	0.7955	1.0709
WOA	1949.8284	33.2691	0.7995	1.1391
DBO	1390.3797	19.5681	0.7935	1.1086

D. Results of Case 4

In this scenario, voltage divergence serves as the goal variable, where a smaller value indicates a better voltage level of the electrical network. Figure 8 shows the trace of the algorithm in case 4. A statistic analysis of the experimental performance for this goal in the selected system is shown in Table X. NOA recorded the lowest mean value of 0.1645 p.u. Table XI shows the optimal solution of NOA compared to the other algorithms, indicating an improvement of 14.14% compared to the average value of the DBO in the second position.

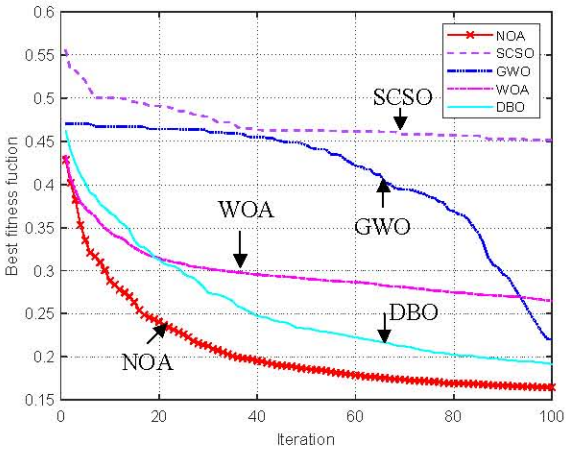

Fig. 8 Iteration curves of each algorithm in Case 4.

TABLE X. OUTCOMES OF EACH ALGORITHM IN CASE 4

Algorithm	Minimum	Maximum	Mean
NOA	0.1511	0.1795	0.1645
SCSO	0.3020	0.6324	0.4512
GWO	0.1796	0.3193	0.2200
WOA	0.1940	0.3505	0.2649
DBO	0.1652	0.2229	0.1916

TABLE XI. COMPARISON OF EACH OBJECTIVE FUNCTION WITH CASE 4 AS THE OPTIMAL OBJECTIVE AND OTHER ALGORITHMS

Algorithm	Fuel cost	Ploss	LKmax	VD
NOA	1231.6607	2.5698	0.9819	0.1511
SCSO	1631.3840	5.4094	0.9691	0.3019
GWO	1705.1089	3.9055	0.9847	0.1796
WOA	944.9224	4.5392	0.9909	0.1940
DBO	1277.6473	5.5797	0.9746	0.1652

VII. CONCLUSION

This research uses the nutcracker optimization algorithm (NOA) to address two optimization problems: CEC2017 function optimization and optimal power flow in the IEEE-30 bus system. The technology effectively minimizes generation expenses,active power loss，steady voltage, and point voltage volatility. Simulation results show NOA's good convergence and robustness, making it a viable option for solving optimal power flow problems.

REFERENCES

[1] B. C. Lesieutre, and I. A. Hiskens. "Convexity of the Set of Feasible Injections and Revenue Adequacy in FTR Markets", *IEEE Transactions on Power Systems*, vol. 20, no. 4, pp. 1790-1798, 2005.

[2] P. N. Biskas, N. P. Ziogos, and A. Tellidou, "Comparison of Two Metaheuristics with Mathematical Programming Methods for the Solution of OPF", *IEE Proceedings-Generation, Transmission and Distribution*, vol. 153, no. 1, pp. 16-24, 2006.

[3] K. Zehar, and S. Sayah, "Optimal Power Flow with Environmental Constraint Using a Fast Successive Linear Programming Algorithm: Application to the Algerian Power System", *Energy Conversion and Management,* vol. 49, no. 11, pp. 3362-3366, 2008.

[4] P. Fortenbacher, and T. Demiray, "Linear/Quadratic Programming-Based Optimal Power Flow Using Linear Power Flow and Absolute Loss Approximations", *International Journal of Electrical Power & Energy Systems*, vol. 107, pp. 680-689, 2019.

[5] S. Mhanna, and P. Mancarella, "An Exact Sequential Linear Programming Algorithm for the Optimal Power Flow Problem", *IEEE Transactions on Power Systems*, vol. 37, no. 1, pp. 666-679, 2021.

[6] R. S. Salgado, and E. L. Rangel, "Optimal Power Flow Solutions through Multi-objective Programming", *Energy*, vol. 42, no. 1, pp. 35-45, 2012.

[7] V. Vasylius, A. Jonaitis, and S. Gudžius, "Multi-period Optimal Power Flow for Identification of Critical Elements in a Country Scale High Voltage Power Grid", *Reliability Engineering & System Safety*, vol. 216, pp. 107959, 2021.

[8] S. Tu, A. Wächter, and E. Wei, "A Two-stage Decomposition Approach for AC Optimal Power Flow", *IEEE Transactions on Power Systems*, vol. 36, no. 1, pp. 303-312, 2020.

[9] M. Pourakbari-Kasmaei, M. Lehtonen, and M. Fotuhi-Firuzabad, "Optimal Power Flow Problem Considering Multiple-fuel Options and Disjoint Operating Zones: A Solver-friendly MINLP Model", *International Journal of Electrical Power & Energy Systems*, vol. 113, pp. 45-55, 2019.

[10] F. Capitanescu, and L. Wehenkel, "Experiments with the Interior-Point Method for Solving Large Scale Optimal Power Flow Problems", *Electric Power Systems Research*, vol. 95, pp. 276-283, 2013.

[11] H. Wei, H. Sasaki, and J. Kubokawa, "An Interior Point Nonlinear Programming for Optimal Power Flow Problems with a Novel Data Structure", *IEEE Transactions on Power Systems*, vol. 13, no. 3, pp. 870-877, 1998.

[12] E. P. De Carvalho, A. Dos Santos Júnior, and T. F. Ma, "Reduced Gradient Method Combined with Augmented Lagrangian and Barrier for the Optimal Power Flow Problem", *Applied Mathematics and Computation*, vol. 200, no. 2, pp. 529-536, 2008.

[13] X. Yuan, B. Zhang, and P. Wang, "Multi-objective Optimal Power Flow Based on Improved Strength Pareto Evolutionary Algorithm", *Energy*, vol. 122, pp. 70-82, 2017.

[14] M. Younes, M. Rahli, and L. Abdelhakem-Koridak, "Optimal Power Flow Based on Hybrid Genetic Algorithm", *Journal of Information Science & Engineering*, vol. 23, no. 6, pp. 1801-1816, 2007.

[15] M. H. Nadimi-Shahraki, S. Taghian, and S. Mirjalili, "EWOA-OPF: Effective Whale Optimization Algorithm to Solve Optimal Power Flow Problem", *Electronicst*, vol. 10, no. 23, pp. 2975, 2021.

[16] M. Ahmad, N. Javaid, and A. Niaz, "A Bio-inspired Heuristic Algorithm for Solving Optimal Power Flow Problem in Hybrid Power System", *IEEE Access*, vol. 9, pp. 159809-159826, 2021.

[17] E. E. Elattar, and S. K. ElSayed, "Modified JAYA Algorithm for Optimal Power Flow Incorporating Renewable Energy Sources Considering the Cost, Emission, Power Loss and Voltage Profile Improvement", *Energy*, vol. 178, pp. 598-609, 2019.

[18] M. A. A. Shaheen, H. M. Hasanien, and A. Al-Durra, "Solving of Optimal Power Flow Problem Including Renewable Energy Resources Using HEAP Optimization Algorithm", *IEEE Access*, vol. 9, pp. 35846-35863, 2021.

[19] S. Khunkitti, A. Siritaratiwa, and S. Premrudeepreechacharn, "A Hybrid DA-PSO Optimization Algorithm for Multiobjective Optimal Power Flow Problems", *Energies*, vol. 11, no. 9, pp. 2270, 2018.

[20] A. Khan, H. Hizam, and N. Bin Abdul Wahab, "Optimal Power Flow Using Hybrid Firefly and Particle Swarm Optimization Algorithm", *Plos One*, vol. 15, no. 8, pp. e0235668, 2020.

[21] M. Abdel-Basset, R. Mohamed, and M. Jameel, "Nutcracker Optimizer: A Novel Nature-inspired Metaheuristic Algorithm for Global Optimization and Engineering Design Problem", *Knowledge-Based System*, vol. 262, pp. 110248, 2023.

[22] O. Alsac, and B. Stott, "Optimal Load Flow with Steady-state Security", *IEEE Transactions on Power Apparatus and Systems*, vol. 3, pp. 745-751, 1974.

[23] N. H. Awad, M. Z. Ali, and P. N. Suganthan, "Ensemble Sinusoidal Differential Covariance Matrix Adaptation with Euclidean Neighborhood for Solving CEC2017 Benchmark Problems", *2017 IEEE Congress on Evolutionary Computation (CEC)*, pp. 372-379, 2017.